Deep phenotyping of peripheral tissue facilitates mechanistic disease stratification in sporadic Parkinson's disease

Phillippa J Carling[1*], Heather Mortiboys[1*], Claire Green[1], Simeon Mihaylov[1], Cynthia Sandor[2], Aurelie Schwartzentruber[1], Rosie Taylor[3], Wenbin Wei[1], Chris Hastings[1], Siew Wong[1], Christine Lo[1], Samuel Evetts[4,5], Hannah Clemmens[1], Matthew Wyles[1], Sam Willcox[1], Thomas Payne[1], Rachel Hughes[1], Laura Ferraiuolo[1], Caleb Webber[2,5], Winston Hide[1,6], Richard Wade-Martins[5,7], Kevin Talbot[4,7], Michele T. Hu[4,5], Oliver Bandmann[1]

*Both authors contributed equally to this manuscript

[1]Sheffield Institute for Translational Neuroscience (SITraN), University of Sheffield, 385a Glossop Road, Sheffield S10 2HQ, UK; [2]UK Dementia Research Institute, Cardiff University, Hadyn Ellis Building, Maindy Road, Cardiff, CF24 4HQ, UK; [3]Statistical Service Unit (SSU), University of Sheffield, UK; [4]Nuffield Department of Clinical Neurosciences, Level 3, Department of Neurology, West Wing, John Radcliffe Hospital, Oxford OX3 9DU, UK; [5]Oxford Parkinson's Disease Centre, University of Oxford, UK; [6]Beth Israel Deaconess Medical Center, Department of Pathology (Dana 519), 330 Brookline Ave, Boston, MA 02215, USA; [7]Department of Physiology, Anatomy and Genetics, University of Oxford, South Parks Road, OX1 3QX UK.

Corresponding author: Prof Oliver Bandmann, MD PhD FAAN, Sheffield Institute for Translational Neuroscience (SITraN), University of Sheffield, 385a Glossop Road, Sheffield S10 2HQ, UK; Tel: x44-114-2222261; email: o.bandmann@sheffield.ac.uk

Abstract:

Mechanistic disease stratification will be crucial to develop a precision medicine approach for future disease modifying therapy in sporadic Parkinson's disease (sPD). Mitochondrial and lysosomal dysfunction are key mechanisms in the pathogenesis of sPD and therefore promising targets for therapeutic intervention. We investigated mitochondrial and lysosomal function in skin fibroblasts of 100 sPD patients and 50 age-matched controls. A combination of cellular assays, RNA-seq based pathway analysis and genotyping was applied. Distinct subgroups with mitochondrial (mito-sPD) or lysosomal (lyso-sPD) dysfunction were identified. Mitochondrial dysfunction correlated with reduction in complex I and IV protein levels. RNA-seq based pathway analysis revealed marked activation of the lysosomal pathway with enrichment for lysosomal disease gene variants in lyso-sPD. Conversion of fibroblasts to induced neuronal progenitor cells and subsequent differentiation into tyrosine hydroxylase positive neurons confirmed and further enhanced both mitochondrial and lysosomal abnormalities. Treatment with ursodeoxycholic acid improved mitochondrial membrane potential and intracellular ATP levels even in sPD patient fibroblast lines with comparatively mild mitochondrial dysfunction. The results of our study suggest that in-depth phenotyping and focussed assessment of putative neuroprotective compounds in peripheral tissue are a promising approach towards disease stratification and precision medicine in sPD.

Key words:

Parkinson's disease, disease stratification, fibroblasts, ursodeoxycholic acid, UDCA.

1. Introduction

Parkinson's disease (PD) continues to be a relentlessly progressive disorder. The failure of previous clinical trials investigating putative neuroprotective compounds for PD may be due to differences between patients in the underlying pathogenic mechanisms. Precision medicine is increasingly advocated as a promising strategy in the pursuit of neuroprotection in PD but would require the identification of distinct pathomechanisms in individual patients (Espay *et al.*, 2017).

We and others have identified distinct abnormalities of mitochondrial or lysosomal function and morphology in peripheral tissue of genetically stratified PD patient cohorts (Hockey *et al.*, 2015; Mortiboys *et al.*, 2010; Mortiboys *et al.*, 2008; Rakovic *et al.*, 2011). Other groups have used PD-patient derived fibroblasts to demonstrate mitochondrial dysfunction in patients with more complex forms of Mendelian PD such as *VPS13C* (Lesage *et al.*, 2016) to investigate the interaction of PD genes such as the role of LRRK2 in the regulation of PINK1/Parkin-dependent mitophagy (Bonello *et al.*, 2019) or to study the physiological role of then newly discovered genes such as ATP13A2 (Dehay *et al.*, 2012). We subsequently undertook the first drug screen in genetically stratified PD patient tissue and identified ursodeoxycholic acid (UDCA) as a promising novel neuroprotective compound (Mortiboys *et al.*, 2013; Mortiboys *et al.*, 2015). Similarly, a fibroblast-based approach was used to demonstrate that ambroxol increases glucosylceramidase activity in the tissue of PD patients with and without heterozygous glucocerebrosidase (*GBA1*) mutations (McNeill *et al.*, 2014). Mitochondrial and lysosomal dysfunction are also key pathogenic mechanisms in sporadic PD (sPD) and therefore particularly promising therapeutic targets (Schapira *et al.*, 2014; van der Brug *et al.*, 2015). We hypothesised that mechanistic stratification for mitochondrial or lysosomal dysfunction in sPD peripheral tissue would allow the identification of mechanistically rather than clinically defined sPD subgroups. The proposed tissue-based mechanistic stratification would facilitate a future

precision medicine approach which may dramatically enhance the likelihood of successful neuroprotection trials in mechanistically stratified sPD.

_____

Abbreviations: GBA, glucocerebrosidase; DA, dopaminergic; DMEM, Dulbecco's Modified Eagle's medium; iNPC, induced neuronal progenitor cells; LRRK2, leucine-rich repeat kinase 2; LSD, lysosomal storage disorder; lyso-PD, subgroup of PD patients with lysosomal dysfunction; mitochondrial membrane potential, MMP; mito-PD, subgroup of PD patients with mitochondrial dysfunction; Parkinson's disease, PD; UDCA, ursodeoxycholic acid.

2. Materials and Methods

2.1. Participant recruitment

Participants were recruited from the Oxford Parkinson's Disease Centre Discovery cohort (22 control and 63 sPD patient participants (Szewczyk-Krolikowski *et al.*, 2014), and from Sheffield Teaching Hospitals through the Sheffield Institute of Translational Neuroscience (SITraN) (28 control and 37 sPD patient participants). Skin punch biopsies were taken from participants with PD and healthy age-matched controls. The study was approved by the respective local institutional review boards. Written informed consent was obtained from all research participants included in this study.

There was no difference in mean age between control and sPD participants (age in years ± standard deviation (SD): sPD patients 61±10.7 years; controls, 61±13.1 years). The average age of disease onset in sPD patients was 58±11.3 years, with an average disease duration of 4.26±3.65 years. All patients and controls were screened for four common Mendelian mutations associated with late onset PD: $LRRK2^{G2019S}$ and $LRRK2^{R1441C/G}$ as well as GBA^{N370S} and GBA^{L444P}. Three out of 100 patients were identified as mutation carriers, carrying $LRRK2^{G2019S}$, GBA^{N370S} or GBA^{L444P}, respectively.

Subsequent in-depth functional experiments were undertaken in the five sPD patients with the most marked reduction in ATP levels (mito-sPD) and also in the five patients with the most marked increase in the number of lysosomes (lyso-sPD). These stratified patient groups were matched with those control participants who were most closely age matched within the cohort. There was no difference in mean age for either the mito-sPD or the lyso-sPD group and the age-matched control groups (mito-sPD patients 60±6.0 years (n=5) and matched controls 62±6.5 years (n=5); lyso-sPD patients 65±11.5 years (n=5) and matched controls 61±10.9 years (n=5). In addition we selected a group of 3 sPD patient fibroblast lines to convert into iNPC's; the iNeuron sub group; these sPD patients were selected based upon having a mixed

mitochondrial and lysosomal profile in fibroblasts; where both mitochondrial and lysosomal measurements were at least 2 SD outside of the control mean. The selection process of the controls was solely based on best-possible age-matching without taking the results from the screening assays for mitochondrial/lysosomal function into account.

2.2. Fibroblast culture

Primary fibroblast cells were cultured continuously in high glucose (4500 mg/L) Dulbecco's Modified Eagle's medium (DMEM; Sigma-Aldrich) supplemented with 10% fetal bovine serum (Sigma-Aldrich), 100 IU/mL penicillin, 100 µg/mL streptomycin (Lonza), 1 mM sodium pyruvate (Sigma-Aldrich) and 50 µg/mL uridine (Alfa Aesar). Unless otherwise stated, 48 hours prior to analysis, the glucose-containing media was exchanged for glucose-free DMEM (Gibco) with the same supplementation and in addition, 5 mM galactose (Sigma-Aldrich). All cells were assessed between passage 6-10.

2.3. Mitochondrial function

The mitochondrial membrane potential (MMP) and total cellular ATP levels were assessed as described previously (Mortiboys et al. 2008). The activity of the mitochondrial complexes I, II and IV were measured in fibroblasts using microplate activity assays (Abcam; ab109721, ab109910, ab109908). The assays were performed according to the manufacturer's instructions using 20-30 µg protein per well for each complex measurement. Complex activity readings were normalised to protein content. Sample protein concentrations were measured using the Pierce BCA Protein Assay Kit (#23227, Thermofisher).

Mitochondrial complex protein content was determined by western blot. Cell pellets from fibroblasts were lysed in RIPA buffer (R0278, Sigma-Aldrich) on ice for 30min. Protein concentration of lysates was determined using Bradford reagent. After SDS-PAGE, protein

was transferred on PVDF. Membranes were probed with mouse total OXPHOS antibodies (a combination of antibodies against Complex I - NDUFB8 subunit; Complex II - SDHB subunit; Complex III - UQCRC2 subunit; Complex IV - COX2 subunit; and Complex V - ATP5A subunit; 1:1,000; ab110411, Abcam); rabbit anti-beta-Actin (1:5,000; ab8227, Abcam) used as a loading control; followed by incubation in secondary rabbit or mouse HRP-conjugated antibodies (1:10,000; Rabbit: Bio-Rad 1706515, Mouse: Bio-Rad1706516; Bio-Rad).

2.4. Lysosomal function

Fibroblasts were incubated for 1 hour with 100 nM LysoTracker® (Life Technologies) and 10 µM Hoechst 33342 (Sigma-Aldrich). Images were captured on the IN Cell Analyzer 2000 and analysed using the paired Developer software (GE Healthcare) allowing for segmentation of lysosomes, nuclei and cell boundaries to quantify lysosomal parameters per cell. Subsequent validation of the LysoTracker-based lysosomal quantification was undertaken using LAMP2 immunocytochemistry. Fibroblasts were fixed in 4% paraformaldehyde, permeabilized with 0.01% Triton X-100 in TBS-T and incubated in primary mouse-Lamp2 antibody (18822, Santa Cruz), then with 488 anti-mouse secondary antibody (A-11001, Life Technologies). Lysosomal function was assessed by quantifying Cathepsin D activity, using a fluorometric assay kit (ab65302, Abcam) and following the user instructions. The lysis buffer supplied by Abcam was substituted for RIPA buffer (R0278, Sigma-Aldrich). Fluorescence signal was measured using Omega FLUOStar plate reader (BMG Labtech). Protein concentration was determined using Pierce™ BCA protein assay kit (23225, ThermoFisher). Cathepsin D activity slope was produced as a function of fluorescence per mg total protein.

2.5. Differential gene expression analysis

500 ng of high quality total RNA, with an RNA integrity number (RIN) of 9 or above, was used in the preparation of sequencing libraries using the NEB Ultra II Directional RNA Library Prep Kit (NEB catalogue number E7760), following the polyA mRNA workflow. Libraries were individually indexed and pooled for standard Illumina sequencing on the HiScan SQ platform. RNA-seq samples were pre-processed with RNA-seq pipeline bcbio (https://github.com/bcbio/bcbio-nextgen) using Salmon quantification (Patro *et al.*, 2017) . Salmon counts for each transcript were rounded to the nearest integer, and passed through the R package DESeq2 to calculate differential gene expression. For both lysosomal and mitochondrial conditions, patient samples were compared against controls. The threshold for differential expression was set at adjusted p value < 0.05. Similarity between patient groups was assessed by gene overlap. Identification of PD-associated genes was conducted using the web tool VarElect (Stelzer *et al.*, 2016) (ve.genecards.org) using the search term "Parkinson's Disease" and either "mitochondria" or "lysosome" depending on the source of the input. Pathway enrichment of DEGs was conducted using the web interface *EnrichR* (Kuleshov *et al.*, 2016).

2.6. Genetic analysis

144 research participants were successfully genotyped using the NeuroChip array. The NeuroChip array described by Blauwendraat C et al. (Blauwendraat *et al.*, 2017) is based on a genome-wide genotyping array (Infinium HumanCore-24 v1.0) containing 306,670 tagging variants and a custom content that has been updated and extended with neurodegenerative disease-related custom content consisting of 179,467 variants. Quality control was carried out using plink (v1.90b3) (Purcell *et al.*, 2007). To call genotypes from the raw data files imported into GenomeStudio (2.0), sample number was sufficient to generate robust clusters within a

larger cohort including 1679 samples and thus no pre-made cluster file was used. 4 samples were excluded for technical reasons. Among the remaining 146 individuals, we discarded two individuals with elevated missing data rates (> 3%), outlying heterozygosity rate (> 3 standard deviation) or for which the gender was unable to be imputed from genotype information on the X chromosome. Finally, we excluded calling genotypes for 11,913 variant positions with high missing date rate (>5%) or that did not pass Hardy-Weinberg test (p value < 10-5). The frequency of all putative damaging variants (category 2b: MAF<3%, CADD C-Score> 12.37) among 51 lysosomal disease (LSD) genes (Robak *et al.*, 2017) was compared between patients and controls, using Fisher's exact test. One patient with a *LRRK2^{G2019S}* mutation was removed from further analysis. The NeuroChip array analysis did not identify any additional relevant changes in Mendelian PD genes (see Supplementary Table 1, PD gene variants). The complete, individualised data of the genetic analysis are not publicly available due to the risk of patient/research participant identification but they are available from the corresponding author on reasonable request.

2.7. Generation of TH-positive neurons and measurement of MMP, cellular ATP levels and lysosomal number

iNPC's were generated from 3 sPD patient fibroblasts and 3 controls (age +/- SD; controls 54.3 +/- 4; sPD 52.3 +/-3; each group comprised of 2 males and 1 female donor) as previously described (Meyer et al, 2014). iNPC's were maintained in DMEM/Ham F12 (Invitrogen); N2, B27 supplements (Invitrogen) and FGFb (Peprotech) in fibronectin (Millipore) coated tissue culture dishes and routinely subcultured every 2-3 days using accutase to detach them. For the generation of TH-positive neurons, iNPCs were plated in a 6-well plate and cultured for 2 days in DMEM/F-12 medium with Glutamax supplemented with 1%NEAA, 2%B27 (Gibco) and

2.5µM of DAPT. On day 3, DAPT was removed and the medium was supplemented with 1µM smoothened agonist (SAG) and FGF8 (75ng/ml) for additional 10 days. Subsequently SAG and FGF8 were withdrawn and replaced with BDNF (30 ng/ml), GDNF (30 ng/ml), TGF-b3 (2 mM) and dcAMP (2 mM, Sigma) for 15 days. In order to verify generation of DA neurons, immunocytochemistry was performed. Cells were plated into 96 well plates and fixed using 4% paraformaldehyde for 30 minutes. After PBS washes, cells were permeabilised using 0.1% Triton X-100 for 10 minutes and blocked using 5% goat serum for 1 hour. Cells were incubated with primary antibodies (tyrosine hydroxylase (Abcam); β III tubulin (Millipore); at 4 degrees for 16 hours. Cells are washed using PBS-Tween and incubated with Alexa Fluor conjugated secondary antibodies 488 and 568 (Invitrogen) and Hoescht (Sigma) 1µM prior to imaging. Imaging was performed using the Opera Phenix high content imaging system (Perkin Elmer). Neurons were incubated with 0.1mg/ml Neurosensor 521 for 30 minutes before removal and of the dye and imaging using high content imager InCell 2000 using green excitation and emission filters.

At end stage of differentiation neurons were plated in 96 well plates (10,000 neurons per well); for live imaging cells were incubated for one hour at 37º with 80 nM tetramethlyrhodamine, (TMRM), 100nM LysoTracker Green (Life Technologies) and Hoescht (Sigma) at 1µM before imaging using Opera Phenix. Twenty fields of view were imaged, in 7 z planes. Images were analysed using Harmony software (Perkin Elmer) using maximal z projections. Mitochondria and lysosomes were segmented and the intensity of the mitochondrial signal was normalised to the total area of cells in a particular field of view. Cellular ATP measurements were undertaken using ATPLite kit (Perkin Elmer) as per manufacturer's instructions.

2.8. Drug treatment

A sub-group of patients with mild mitochondrial impairment (either ATP levels (n=3) or MMP levels (n=3) > 2 SD but < 3SD below the mean of the control cohort respectively) were assessed after treatment with UDCA. The average age of these otherwise randomly selected six sPD patients was 53±2.5 years, the average age of the matched controls was 54±4.0 years. 24 hours before assaying fibroblasts were changed into galactose media containing either DMSO only or 10uM UDCA to determine the effect on MMP, intracellular ATP levels and complex I/IV activity (see above).

2.9. Statistics

Values from multiple experiments were expressed as mean +/- SD. Statistical analysis was performed using GraphPad Prism. Individual parameters were assessed with two-tailed unpaired t-tests apart from untreated versus treated groups which were compared using a paired t test due to the 1:1 matching on age. Mann Whitney U non-parametric test was used between control and sPD selected groups where the assumption of normality was not valid. Correlation was determined using Pearson's correlation coefficients. Statistical significance in grouped analyses were assessed using two-way ANOVA with Bonferroni post hoc correction. Variances were compared using an F-test. All data was expressed as % of controls unless otherwise stated. Comparisons were declared to be statistically significant at a 5% significance level, as this is an exploratory, hypothesis generating study no adjustment was made for multiple testing.

3. Results

3.1. Mitochondrial function

There was no overall difference in sample means between the entire sPD cohort and the control group for either ATP (patients 100.84±12.48, controls 100.76±6.76; p=0.97) or MMP (patients 106.89±22.49, controls 100.84±14.99; p=0.087). However, as can be seen from Figs 1A and 1B, the variability in ATP and MMP was larger in sPD patients compared to controls (F-test, p<0.0001 for ATP and p=0.0021 for MMP). In particular 12/100 sPD patients had ATP levels reduced by >2SD with four sPD patients having ATP levels >3SD lower than the control mean (Fig. 1A). 5/100 sPD patients had MMP levels >2SD lower than the mean of the controls (Fig. 1B). Total cellular ATP and MMP were not correlated with age of onset (Fig. 1C, D), or disease duration (Fig. 1E, F). There was also no correlation with age at the time of biopsy (data not shown).

To further characterize the underlying mechanisms leading to impaired mitochondrial function, electron transport chain (ETC) protein levels were assessed via western blotting in the five patients with the most marked decrease in ATP levels (mito-sPD) alongside five closely age-matched controls (see Supplementary Figure 1 for representative Western Blot image). These patients showed a decrease in NDUFB8 (complex I) and COX2 (complex IV) protein levels (NDUF8 - patients 59.73±18.72, controls 100.00±16.8; p<0.05; COX2 – patients 56.93±20.57; controls 100.00±25.42; p<0.05). No differences were observed in the other complexes (complex II/SDHB - patients 72.32±21.15, controls 100.00±19.41; p>0.05; complex III/UQCRC2 - patients 106.73±15.42, controls 100±42.43; p>0.05; complex V/ATP5A - patients 104.33±15.32, controls 100.00±26.41; p>0.05; Fig. 1G). To further evaluate the effect of this decrease, NDUF8 and COX2 protein levels were plotted against ATP levels for each patient and control and correlation coefficients and linear regressions produced. Plots and correlation coefficients suggested that the observed lower ATP levels may at least partially be

due to decreased NDUF8 and COX2 protein levels (NDUF8– $R^2=0.55$; $p<0.05$; COX2 – $R^2=0.46$; $p<0.05$; Fig. 1H).

3.2. Lysosomal dysfunction

Both the number of lysosomes (patients 114.16±36.54; controls 100.36±26.91; $p<0.05$) and their total area (patients 118.13±47.09; controls 101.01±33.08; $p<0.05$) were increased in sPD (Fig. 2A-D). 15/100 sPD patients had a lysosome count >2SD greater than the control average. In a subgroup of patients (lyso-sPD) with lysosome counts >3SD greater than the control mean, confirmatory tests were undertaken, including immunocytochemistry for the lysosomal membrane protein LAMP2 and measurement of Cathepsin D activity. LAMP2 immunocytochemistry confirmed an increase in lysosome number in the assessed patients within the lyso-sPD group (patients (n=5) 135.74±17.63; controls (n=5) 100.00±6.1; $p<0.001$, Fig. 2E). Cathepsin D activity was then correlated with the number of lysosomes. A marked decrease in Cathepsin D activity per lysosome was seen in lyso-sPD, suggesting lysosomal dysfunction (patients 49.62±5.74; controls 100.00±49.79; $p<0.05$, Fig. 2F). The number of lysosomes were not correlated with age at the time of biopsy, age of onset or disease duration (data not shown). Supplementary table 2 summarizes the MMP, ATP and lysosome count number for all research participants.

The change in Cathepsin D activity is specific to the identified lysosomal sub-group as we measured the Cathepsin D activity in the mitochondrial sub-group and found no difference to matched controls (Supplementary Figure 2).

3.3. Pathway analysis

In the two subgroups of sPD patients with either lysosomal count >3SD (lyso-sPD, n=5) or reduced ATP levels >3SD (mito-sPD, n=5), RNAseq-based differential gene expression analysis revealed 342 genes that were differentially expressed in lyso-sPD compared to age-matched controls. Conversely, 84 genes reached significance in mito-sPD. There was no overlap in differentially expressed genes (DEG) between the two subgroups. The top 10 results for the lyso-sPD group from the gene-disease phenotype association tool VarElect (Stelzer *et al.*, 2016) indicate a number of these DEGs have established associations with both PD and the lysosome (Table 1, see also Supplementary Table 3 for complete list of all differentially expressed genes for lyso-sPD vs controls meeting an adjusted p value < 0.05).

Enrichment analysis revealed enrichment for a number of signalling pathways, the KEGG pathways; "TNF signalling" and "Lysosome" were most markedly impaired (Table 2). Of the 10 genes overlapping with this lysosome pathway, 9 were upregulated in patients (Table 3). The single downregulated gene, LITAF, is likely due to zero counts detected for all four patients, which explains its high fold change value.

In contrast, the 84 DEGs associated with mito-sPD did not enrich for any functions or pathways and therefore failed to identify any pathways associated with mitochondrial dysfunction. To identify the presence of an underpowered signal, the p value threshold was relaxed to include genes which only achieved an *unadjusted* p value of <0.05 for both conditions. Six hundred and thirty overlapping genes were removed, leaving 1659 DEGs for VarElect analysis in the mito-sPD group. This exploratory approach identified *SNCA* and *PLA2G6* as the genes with the highest VarElect score (Table 4, see also Supplementary Table 4 for complete list of all differentially expressed genes for mito-sPD vs controls meeting an adjusted p value < 0.05).

3.4. Genetic analysis

Shulman and co-workers had previously reported an excessive burden of gene variants in 54 LSD genes in PD (Robak *et al.*, 2017). We hypothesised that there would be an enrichment of LSD gene variants in the stratified patient cohort which displayed lysosomal dysfunction and related changes in the RNAseq-based pathway analysis. NeuroChip-based genotyping for sequence variants in the same LSD genes previously investigated by Shulman and colleagues (Supplementary Table 5a) did not identify an overall difference in the number of individuals carrying one or more damaging LSD variants between the entire PD cohort and controls (PD: 17/99 carrying one damaging LSD variant (17.2%), one of these PD patients carried a second variant; controls: 7/50 (14%) damaging LSD variants; p value of Fisher's exact test = 0.64). However, the proportion of PD patients carrying an LSD damaging variant rose to 5/14 (35%, p value of Fisher's exact test = 0.060) for the group of patients with a lysosomal count of > 2 SD and to 3/5 (60%, p value of Fisher's exact test = 0.031) in the patients with a lysosomal count of > 3SD (Supplementary Table 5b).

3.5. Mitochondrial and lysosomal abnormalities are confirmed and further exacerbated in TH-positive neurons generated from a subset of sPD patients

TH-positive neurons were differentiated from iNPC's (i-neurons) derived from fibroblasts of 3 sPD patients and 3 controls. We determined the neuronal properties by assessing changing morphology, immunostaining for several neuronal markers and qPCR. The neurons become more elongated and form connections at the later stages of differentiation, as shown by the representative images of a control and sPD line at day 27 of differentiation (Figure 3A (i) and (ii)). We stained for general neuronal markers, β III tubulin and Map2. As can be seen in the

representative images in Figure 3A (iii) and (iv) both control (iii) and sPD (iv) neurons stained positively for βIII tubulin. Figure 3A (v) and (vi) show images for positive staining of a control (v) and sPD (vi) line of Map2. Furthermore we assessed the expression of DA neuron markers such as TH and DAT. Figure 3B (i) and (ii) show representative images of TH staining in a control (i) and sPD (ii) line. Representative images of TH staining for the remaining four i-neuron cell lines are shown in Supplementary Figure 3. The expression level was also quantified; with no difference between the control and sPD (Figure 3B (vi)). In addition, we used qPCR to quantify the TH expression levels in iNPC's and iNeurons. We see a 3.4 fold increase in TH expression in the iNeurons (Figure 3B (v)). In addition to TH we assessed expression of DAT; with representative images shown in Figure 3B (iii) of a control and (iv) for sPD; showing clear overall expression in most cells of both control and sPD.

Fibroblasts from sPD patients within this subgroup had a reduction in cellular ATP levels or MMP of >2SD from the control mean; with a mean reduction in cellular ATP levels in the fibroblasts of 15% and a mean reduction of MMP in the fibroblasts of 21% in this group. Cellular ATP levels in the DA i-neurons were reduced by 59.7% compared to controls (mean +/- SD; controls: 100.1 +/- 33.5; sPD: 40.29 +/- 20.24, ** $p < 0.05$, Figure 3C (iii)). Similarly, MMP quantification also revealed enhanced deficits in the sPD patient derived TH-positive i-neurons with MMP decreased by 44.5% compared to controls (mean +/- SD; controls: 8208 +/- 577; sPD: 4643 +/- 678; *** $p < 0.01$). Example images of the MMP in a control and sPD TH-positive neuron line are shown in Figure 3C (i) and (ii); the intensity of the TMRM signal is clearly reduced in the sPD TH-positive neurons.

We also assessed the lysosomal number in these DA i-neurons; in this group of sPD patient fibroblasts, the lysosome number was increased by 6.5%; whereas in the TH-positive i-neurons derived from the same sPD patient group lysosome number was increased by 71% compared

to controls (% normalised to controls shown as mean +/- SD; controls 100 +/- 22.8; sPD 171.8 +/- 36.4; * $p < 0.05$, Figure 3C (v)).

3.6. Treatment response in stratified patient tissue

Finally, we sought to discover whether UDCA had a recovery effect on mitochondrial respiratory chain function in stratified sPD tissue comparable to the beneficial effect observed in genetically stratified, *parkin* or *LRRK2[G2019S]* mutant tissue (Mortiboys *et al.*, 2013; Mortiboys *et al.*, 2015). UDCA and its taurine conjugate tauroursodeoxycholic acid (TUDCA) are thought to exert a neuroprotective effect via Akt activation (Castro-Caldas *et al.*, 2012; Chun and Low, 2012; Mortiboys *et al.*, 2013). As severe mitochondrial impairment was comparatively rare in the overall sPD patient group, we selected a group of six sPD patient fibroblasts with mildly impaired mitochondrial function (ATP or MMP levels > 2 SD but < 3 SD below the mean of controls) in order to assess the potential of UDCA treatment to be beneficial in a larger patient population. As predicted, treatment of these mechanistically stratified sPD fibroblasts with 10 µM UDCA for 24 hours increased cellular ATP levels up to 103% and MMP up to 92% of control levels (Fig. 4A, B; $p < 0.01$). Individual respiratory chain measurements identified a decrease of 75% in complex I activity (Fig. 4C, $p < 0.001$) and a decrease of 37% in complex IV activity in the selected sPD patients (Fig. 4D, $p < 0.01$). Treatment with UDCA increased both complex I and complex IV activity to 80% of control levels, however this was only significant for complex I activity (Fig. 4C, $p < 0.01$).

4. Discussion

Precision medicine has already become reality in some areas of medical care such as non-small cell lung cancer (Li *et al.*, 2013), where the choice of treatment regime is guided by the specific underlying genetic cause in a given patient. Genetic stratification may be a particularly promising approach for certain subtypes of PD as well, the first phase II drug trials focussing on PD patients carrying *GBA1* mutations are under way (NCT02906020; NCT02914366) (Gasser, 2015). However, genetic stratification is unlikely to be applicable to the majority of PD patients in the UK and elsewhere with only 1% of sPD patients who present at a typical age and carry Mendelian PARK gene mutations (Tan *et al.*, 2019). Doubts whether genetic stratification of common disorders will fulfil the promise of precision medicine have also been cast in other areas of medicine (Joyner and Paneth, 2019). Precision medicine focussing on mechanistically anchored disease subgroups may therefore hold greater promise (Rosen and Zeger, 2019). We now demonstrate the utility of using skin fibroblasts to undertake such mechanistic stratification in sPD. The proposed stratification approach may offer particular value in neuroprotective treatment trials assessing the effect of a mitochondrial or lysosomal rescue agent on disease progression in sPD. However, we acknowledge that larger cohorts need to be assessed to confirm our findings. A further limiting aspect of our approach is the invasive nature of skin biopsies which may limit a potential adaption into routine clinical care. Future studies need to determine whether fibroblasts could be replaced or combined with other, less invasive strategies such as advanced imaging techniques or assessment of mitochondrial function in blood monocytes (Hattingen *et al.*, 2009; Smith *et al.*, 2018).

The absence of any marked group differences (with the possible exception of lysosomal dysfunction) between the entire sPD cohort and the control cohort supports the assumption of aetiological heterogeneity in sPD. The presence of a *LRRK2*^{G2019S} in one patient and of *GBA1* mutations in two further patients did not allow a prediction of their cellular phenotype.

Our results are in keeping with a recently proposed, elegant concept of biomarker-driven phenotypes for sPD (Espay *et al.*, 2017). Espay and co-workers proposed a model of biomarker-defined, homogenous subtypes of PD likely to respond optimally to therapies proven to affect the causative biological processes within each subtype. They suggested a re-evaluation of the biomarker-discovery effort for sPD, using abnormal biological signals (rather than clinical definitions) to define disease phenotypes. Their proposed exploratory approach, based on a systems-biology model with abnormal biological signals defined as >2SD above or below the mean to identify biologically defined subgroups is strikingly comparable to the approach used and the data obtained in our study.

Our RNAseq-based pathway analysis in the lyso-sPD subgroup strongly suggested that the observed lysosomal dysfunction is associated with an upregulation of lysosomal transcriptional networks and identified a number of lysosomal genes/proteins previously associated with PD such as SMPD1 or RAB7A. The increase in the transcript levels of crucial lysosomal genes may be a compensatory mechanism for impaired lysosomal function in the lyso-sPD subgroup, reflected by the reduced Cathepsin D enzymatic activity per lysosome in this group. The noticeable enrichment for LSD gene variants in the lyso-sPD group suggests that the observed lysosomal dysfunction is at least partially driven by genetic factors. However, replication in a considerably larger cohort are required to confirm the apparent association between LSD gene variants and lysosomal dysfunction in peripheral tissue of sPD patients.

In contrast, there was a noticeable absence of pathway enrichment in the RNAseq analysis of the mito-sPD group. This suggests that the observed mitochondrial dysfunction is neither due to transcriptionally regulated pathways nor does the reduced ATP production appear to result in compensatory changes at the transcriptional level. The observed upregulation of *SNCA* and *PLA2G6* as well as other genes such as *APP* (table 4) previously implicated in PD or other neurodegenerative diseases has to be interpreted with caution since these genes were only

upregulated when the p value threshold was relaxed to include genes which achieved an *unadjusted* p value of <0.05. We acknowledge that the observed mitochondrial and lysosomal dysfunction as well as the associated gene expression changes in the lyso-sPD group may only be epiphenomena due to interaction with other biological mechanisms. However, we propose that it is still plausible to assume that patients in the mito-sPD and lyso-sPD subgroups are more likely to benefit from putative neuroprotective compounds focussing on the rescue of mitochondrial or lysosomal function respectively.

Direct conversion of fibroblasts to iNPCs and subsequent differentiation to DA neurons provides a fast methodology to obtain high-yield of specialised neurons from somatic cells while retaining the genetic background of the donor and avoiding the clonal expansion typical for stem-cell derived neurons (Meyer *et al.*, 2014). This significantly improves the reproducibility of the data, as each iNPC line is representative of the donor without having to select or compare individual clones. The confirmation of mitochondrial or lysosomal abnormalities in TH-positive i-neurons derived from sPD fibroblasts is in keeping with the hypothesis that the observed abnormalities in the peripheral tissue would also be present in the brains of the respective sPD patients. To our knowledge, indices of mitochondrial or lysosomal dysfunction in peripheral tissue from sPD patients have never been compared to mitochondrial or lysosomal dysfunction in peripheral tissue-derived inducible TH-positive i-neurons from the same patient. The markedly enhanced abnormalities in the TH-positive i-neurons suggests that even comparatively mild abnormalities in skin fibroblasts may reflect significant impairment in neuronal tissue. The reasons we see the enhanced phenotype in the i-neurons could be due to the metabolic status of the cells; neurons heavily reliant on OXPHOS to maintain energy levels; in addition to the expression of disease relevant proteins such as alpha synuclein in the neurons as opposed to fibroblasts. A similar phenomenon were observed in Friedreich's Ataxia and motor neuron disease (Georges *et al.*, 2019; Vandoorne *et al.*, 2019). Further studies are

necessary to compare and possibly combine the different approaches assessing mitochondrial or lysosomal function in peripheral tissue in sPD (Atashrazm *et al.*, 2018; Papagiannakis *et al.*, 2015; Shamir *et al.*, 2017; Smith *et al.*, 2018). The observation of abnormalities in non-neuronal tissue may reflect strong genetic determinants but is also in keeping with other, more speculative hypotheses such as PD being a generalized metabolic disorder which predominantly affects (but is not limited to) DA neurons.

We predict that *ex vivo* testing of putative neuroprotective compounds in individual sPD patient tissue (fibroblasts, i-neurons or alternative approaches) will soon become a routine part of the initial triaging process for mechanistically defined multi-arm neuroprotection trials in sPD. The beneficial effect of UDCA in sPD patient tissue reported here is comparable to the effect we previously observed in genetically stratified PD patient tissue (Mortiboys *et al.*, 2013; Mortiboys *et al.*, 2015). We are now undertaking a phase II, proof of concept study to establish safety and tolerability of UDCA at a dose of 30 mg/kg in sPD and explore its neuroprotective potential (clinicaltrials.gov NCT03840005).

In conclusion, we acknowledge that our work has only identified distinct pathomechanisms in some but not all sPD fibroblast lines. However, our data nevertheless suggest that in-depth phenotyping of peripheral tissue can be helpful in moving towards mechanistic disease stratification and precision medicine approaches in sPD.

Declaration of interest

None.

Acknowledgements

Tables:

Gene Symbol	Gene Name	Matched Phenotypes	VarElect Score
CTSD	Cathepsin D	Parkinson's Disease, Lysosome	59.51
SMPD1	Sphingomyelin Phosphodiesterase 1	Parkinson's Disease, Lysosome	56.85
FUCA1	Alpha-L-Fucosidase 1	Parkinson's Disease, Lysosome	45.44
NPC1	NPC Intracellular Cholesterol Transporter 1	Parkinson's Disease, Lysosome	42.31
MAPK3	Mitogen-Activated Protein Kinase 3	Parkinson's Disease, Lysosome	34.54
RAB7A	RAB7A, Member RAS Oncogene Family	Parkinson's Disease, Lysosome	29.89
IGF2	Insulin Like Growth Factor 2	Parkinson's Disease, Lysosome	23.58
ALDH1A1	Aldehyde Dehydrogenase 1 Family Member A1	Parkinson's Disease	21.85
MSX1	Msh Homeobox 1	Parkinson's Disease	19.67
SORT1	Sortilin 1	Parkinson's Disease, Lysosome	18.28

Table 1: Top 10 results for lysosomal-dysfunctional DEGs from VarElect. Investigation of DEGs using online tool VarElect with the terms "Lysosome" and "Parkinson's Disease" indicates a number of genes score highly for association with these terms. *Gene symbol* represents official HGNC symbol. *Matched Phenotypes* indicates the terms inputted into VarElect which have been associated with each gene. Results are ranked by the VarElect score.

Term	Overlap	P-value	Adjusted P-value	Genes
TNF signaling pathway	10/110	0.0000199	0.004103	MAP2K3, NFKBIA, IKBKB, TAB2, CXCL1, CXCL3, PTGS2, IL18R1, CXCL5, MAPK3
Lysosome	10/123	0.0000551	0.005396	PLA2G15, CD63, ATP6V0B, NPC1, SORT1, FUCA1, SMPD1, LITAF, CTSD, ATP6V0A1
Small cell lung cancer	8/86	0.0001122	0.007545	NFKBIA, ITGB1, IKBKB, CDKN1B, ITGA3, FN1, ITGA6, PTGS2
Circadian rhythm	5/30	0.0001442	0.007545	PER1, CSNK1D, NR1D1, CSNK1E, ARNTL
Rap1 signaling pathway	12/211	0.0002922	0.010408	MAP2K3, ITGB1, KITLG, PLCB4, PRKD3, PDGFD, ITGB2, GNAS, RAPGEF5, RAPGEF6, FGF2, MAPK3

Table 2: Top 5 most enriched KEGG pathways for lysosome-dysfunctional DEGs.

Results indicate an enrichment of signalling pathways as well as the pathway "Lysosome".

Overlap indicates number of genes in input list/total number of genes in pathway list.

"Genes" lists the DEGs present in each pathway.

Gene Symbol	Gene Name	Fold Change	P Value	Adjusted P Value
PLA2G15	Phospholipase A2 Group XV	1.67	7.56E-15	1.06E-10
CTSD	Cathepsin D	2.54	1.80E-07	0.00017135
FUCA1	Alpha-L-Fucosidase 1	2.89	2.12E-05	0.0075658
SMPD1	Sphingomyelin Phosphodiesterase 1	1.89	5.65E-05	0.01389979
ATP6V0B	ATPase H+ Transporting V0 Subunit B	1.62	7.09E-05	0.01636507
CD63	CD63 Molecule	1.69	0.00011924	0.02430102
LITAF	Lipopolysaccharide Induced TNF Factor	-142.71	0.00012847	0.02535096
ATP6V0A1	ATPase H+ Transporting V0 Subunit A1	1.73	0.00013745	0.02665443
SORT1	Sortilin 1	3.71	0.00020504	0.03480873
NPC1	NPC Intracellular Cholesterol Transporter 1	3.26	0.00021755	0.03554635

Table 3: Fold change and P-values for the 10 DEGs which enrich within the KEGG pathway "Lysosome". Upregulation of expression was observed for most genes except the gene *LITAF* which shows downregulation. P Values and Adjusted P Values are as reported from DESeq2 analysis.

Gene Symbol	Gene Name	Matched Phenotypes	VarElect Score
SNCA	Synuclein Alpha	Parkinson's Disease, Mitochondria	318.70
PLA2G6	Phospholipase A2 Group VI	Parkinson's Disease, Mitochondria	99.07
RPS27A	Ribosomal Protein S27a	Parkinson's Disease, Mitochondria	63.08
PODXL	Podocalyxin Like	Parkinson's Disease, Mitochondria	53.55
NDUFS2	NADH:Ubiquinone Oxidoreductase Core Subunit S2	Parkinson's Disease, Mitochondria	52.91
GCH1	GTP Cyclohydrolase 1	Parkinson's Disease, Mitochondria	52.80
APP	Amyloid Beta Precursor Protein	Parkinson's Disease, Mitochondria	49.75
PANK2	Pantothenate Kinase 2	Parkinson's Disease, Mitochondria	49.62
NDUFS1	NADH:Ubiquinone Oxidoreductase Core Subunit S1	Parkinson's Disease, Mitochondria	48.41
NDUFAF5	NADH:Ubiquinone Oxidoreductase Complex Assembly Factor 5	Parkinson's Disease, Mitochondria	43.05

Table 4: Top 10 results for unadjusted mitochondrial-dysfunctional DEGs from VarElect. Investigation of DEGs using online tool VarElect with the terms "Mitochondria" and "Parkinson's Disease" in mito-sPD compared to controls indicates a number of genes score highly for association with these terms, including well-established PD genes. *Gene symbol* represents official HGNC symbol. *Matched Phenotypes* indicates the terms inputted into VarElect which have been associated with each gene. Results are ranked by VarElect score.
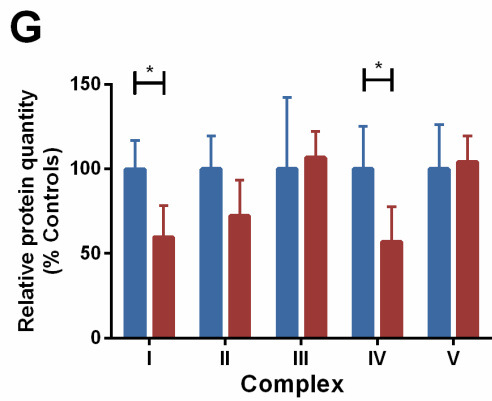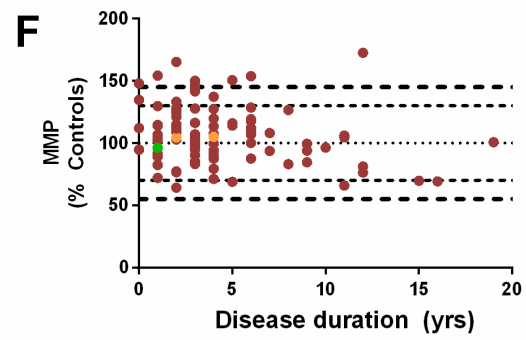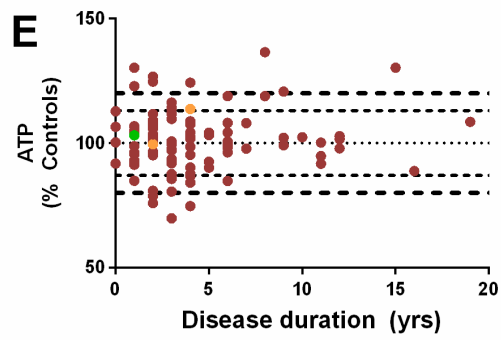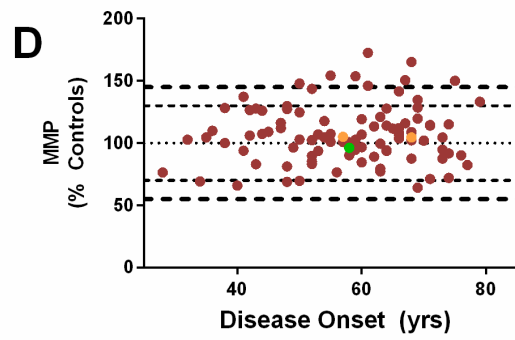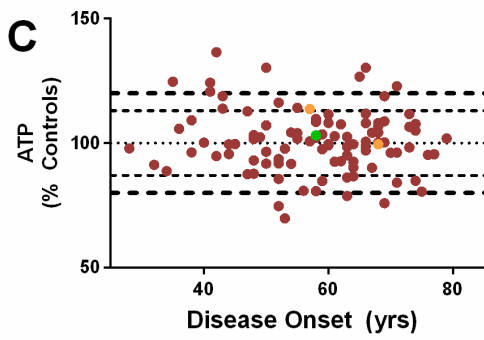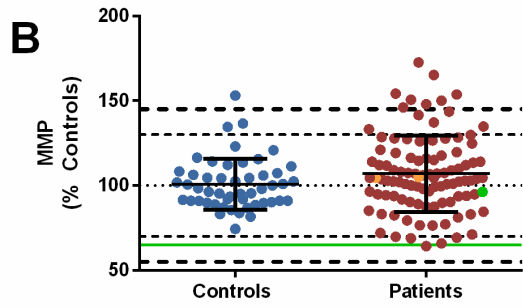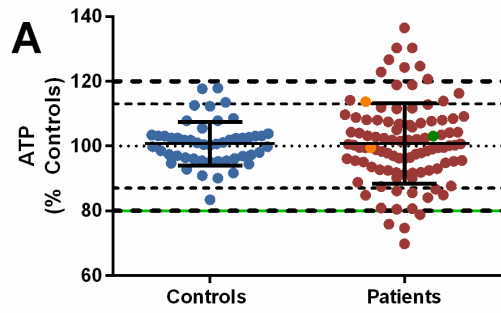
Figures:
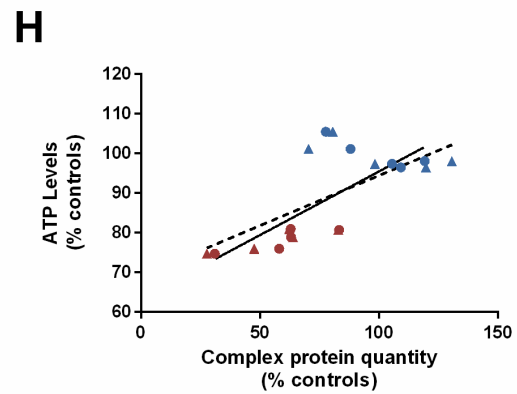
Figure 1: Cellular ATP and mitochondrial membrane potential in sPD patients. Total cellular ATP levels (**A**) and mitochondrial membrane potential (MMP) (**B**) in 100 sPD patients (red circles) and age-matched control participants (blue circles). 12 sPD patients had ATP levels > 2SD (fine dashed line) lower than controls with ATP levels > 3 SD (thick dashed line) in four of these sPD patients. The sPD patient carrying a *LRKK2*^{*G2019S*} mutation is depicted with a green circle, the two patients carrying *GBA1* mutations are depicted with orange circles (**A, B**). The average ATP and MMP levels previously detected in *LRKK2*^{*G2019S*} mutant fibroblasts are indicated for comparison with a green line (Mortiboys et al. 2010). Neither ATP (**C,E**) nor MMP (**D, F**) correlated with either age at disease onset or disease duration since diagnosis, (**G**) NDUFB8 (complex I) and COX2 (complex IV) protein levels were reduced in the subset of the five sPD patients with the lowest intracellular ATP levels compared to age-matched controls (NDUFB8 - sPD 59.73±18.72, controls 100±16.8; $p<0.05$; COX2 – sPD 56.93±20.57; controls 100±25.42; $p<0.05$). In contrast, complex II/SDHB (sPD 72.32±21.15, controls 100±19.41; $p>0.05$; complex III/UQCRC2 (sPD 106.73±15.42, controls 100±42.43; $p>0.05$) and complex V/ATP5A (sPD 104.33±15.32, controls 100±26.41; $p>0.05$) protein levels were normal. (**H**) The observed reduction in NDUFB8/Complex I (circles/solid line) and COX2/complex IV (triangle/dashed line) protein levels correlated with the reduction in ATP levels (NDUF8– $R^2=0.55$; $p<0.05$; COX2 – $R^2=0.46$).
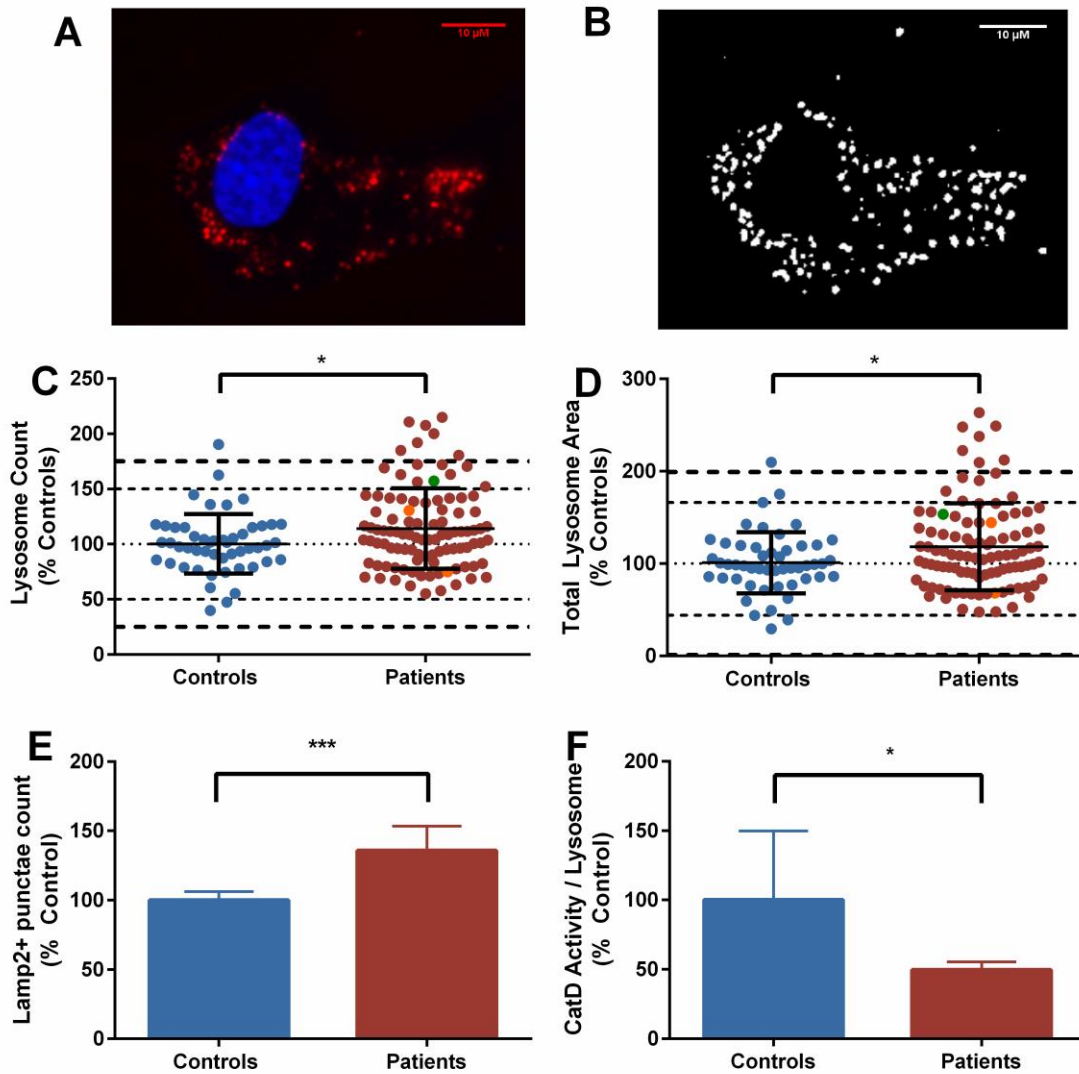
Figure 2: Assessing lysosomes in sPD patients. The number and area of lysosomes were quantified in sPD patients (n=100; red circles) and age-matched control participants (n=50; blue circles) by (**A**) staining fibroblasts with LysotrackerRed (lysosomes; red) and Hoechst (nuclei; blue) with subsequent (**B**) segmented image analysis using the Developer software (scale bar = 10μM). Both the number of lysosomes (sPD 114.2±36.54; controls 100.4±26.91; $p < 0.05$, **C**) and their total area (sPD 118.1±47.09; controls 101.0±33.08; * $p < 0.05$, **D**) were increased in sPD (thin dashed line – 2SD; thick dashed line – 3SD). The sPD patient carrying a *LRKK2*[G2019S] mutation is depicted with a green circle, the two patients carrying *GBA1* mutations are depicted with orange circles. LAMP2 immunocytochemistry confirmed an

increase in lysosome number in the five sPD patients with the most marked increase in lysosome number (sPD 135.74±17.63; controls 100±6.1; *** p<0.001, **E**). In contrast, Cathepsin D activity was decreased, suggesting lysosomal dysfunction with compensatory increase in number (sPD 49.62±5.74; controls 100±49.79; * p<0.05, **F**).
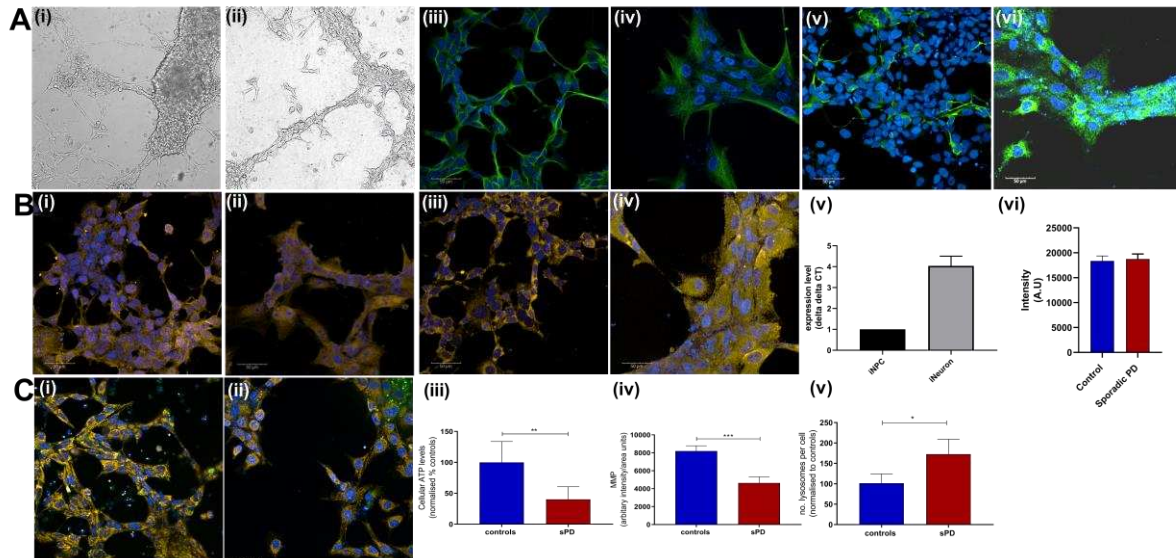
Figure 3: (A) Characterisation of fibroblast-derived TH-positive neurons. Representative images of control (i, iii, v) and sPD (ii, iv, vi) derived TH-positive neurons at the end stage of differentiation brightfield (i) and (ii); stained for βIII tubulin (green) and Hoechst (nuclei, blue; iii and iv) and Map2 (green) and Hoechst (nuclei, blue; (v and vi)).

(**B**) Representative images of control (i;iii) and sPD (ii;iv) neurons at the end stage of differentiation stained for tyrosine hydroxylase (red) and Hoechst (nuclei, blue i and ii). Panels (iii) and (iv) have been stained with DAT (red), Hoechst (nuclei, blue). (v) TH mRNA expression was assessed in iNPC's and end stage iNeurons, showing a 3.4 fold increase in TH expression. (vi) TH expression levels were quantified from controls and sPD iNeurons, with no differences found.

(**C**) Panels (i) and (ii) show representative images of TMRM stained mitochondria and lysotracker stained lysosomes in iNeurons from a control (i) and an sPD patient (ii) (red is mitochondria, green is lysosomes and blue nuclei). (iii) Cellular ATP levels are reduced by 59.7% in sPD dopaminergic neurons, ** $p < 0.05$. (iv) MMP is similarly reduced in sPD dopaminergic neurons by 44.5%, *** $p < 0.01$. (v) Lysosome number is increased in sPD

dopaminergic neurons by 71%, * p < 0.05. Neurons were differentiated from 3 controls and 3

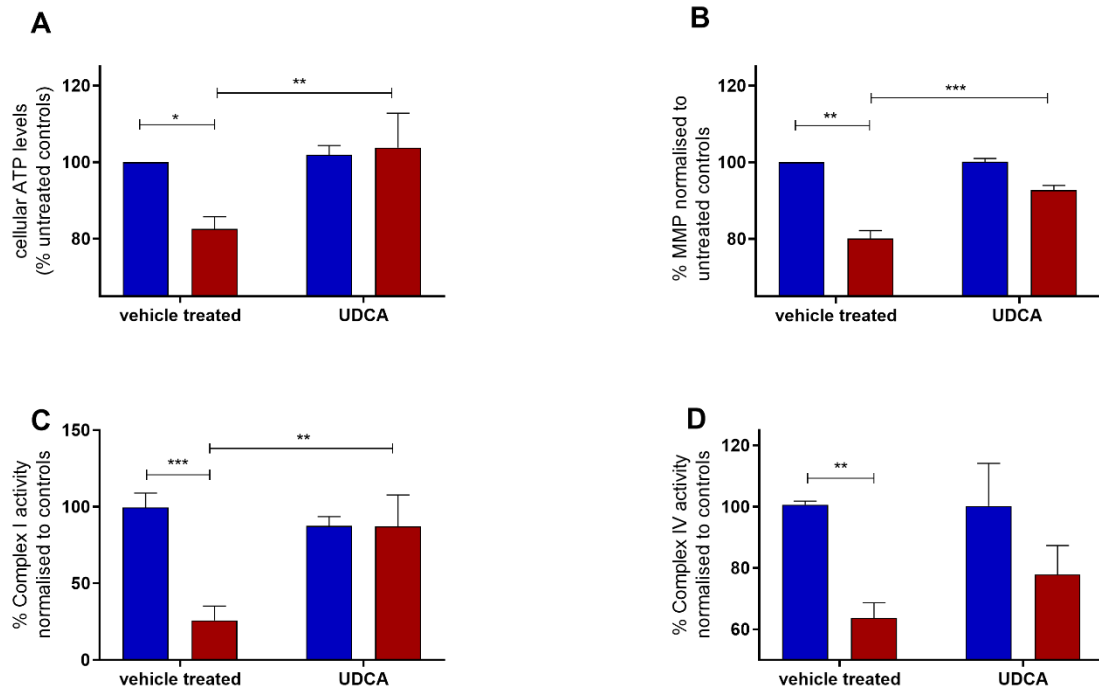sPD patients on at least 3 rounds of differentiation. Scale bar is 50µm.

Figure 4: Recovery of mitochondrial deficits after UDCA treatment in sPD patient fibroblasts. (A) UDCA treatment increases cellular ATP in sPD fibroblasts (red bars, n=6) to 103% of control levels (blue bars, n=6, ** p < 0.01) and **(B)** the mitochondrial membrane potential (MMP) to 92% of controls (*** p < 0.001). **(C)** Individual respiratory chain measurements identified a decrease of 75% in complex I activity (*** p < 0.001) and **(D)** a decrease of 37% in complex IV activity (** p < 0.01) in the selected sPD patient fibroblasts lines. Treatment with UDCA increased both complex I **(C)** and complex IV **(D)** activity to 80% of control levels however this was only significant for complex I activity (** p < 0.01).

References:

Atashrazm, F., Hammond, D., Perera, G., Dobson-Stone, C., Mueller, N., Pickford, R., Kim, W.S., Kwok, J.B., Lewis, S.J.G., Halliday, G.M., Dzamko, N., 2018. Reduced glucocerebrosidase activity in monocytes from patients with Parkinson's disease. *Sci Rep* 8**,** 15446.

Blauwendraat, C., Faghri, F., Pihlstrom, L., Geiger, J.T., Elbaz, A., Lesage, S., Corvol, J.C., May, P., Nicolas, A., Abramzon, Y., Murphy, N.A., Gibbs, J.R., Ryten, M., Ferrari, R., Bras, J., Guerreiro, R., Williams, J., Sims, R., Lubbe, S., Hernandez, D.G., Mok, K.Y., Robak, L., Campbell, R.H., Rogaeva, E., Traynor, B.J., Chia, R., Chung, S.J., International Parkinson's Disease Genomics Consortium, C.-P.D.C., Hardy, J.A., Brice, A., Wood, N.W., Houlden, H., Shulman, J.M., Morris, H.R., Gasser, T., Kruger, R., Heutink, P., Sharma, M., Simon-Sanchez, J., Nalls, M.A., Singleton, A.B., Scholz, S.W., 2017. NeuroChip, an updated version of the NeuroX genotyping platform to rapidly screen for variants associated with neurological diseases. *Neurobiol Aging* 57**,** 247 e249-247 e213.

Bonello, F., Hassoun, S.M., Mouton-Liger, F., Shin, Y.S., Muscat, A., Tesson, C., Lesage, S., Beart, P.M., Brice, A., Krupp, J., Corvol, J.C., Corti, O., 2019. LRRK2 impairs PINK1/Parkin-dependent mitophagy via its kinase activity: pathologic insights into Parkinson's disease. *Hum Mol Genet* 28**,** 1645-1660.

Castro-Caldas, M., Carvalho, A.N., Rodrigues, E., Henderson, C.J., Wolf, C.R., Rodrigues, C.M., Gama, M.J., 2012. Tauroursodeoxycholic acid prevents MPTP-induced dopaminergic cell death in a mouse model of Parkinson's disease. *Mol Neurobiol* 46**,** 475-486.

Chun, H.S., Low, W.C., 2012. Ursodeoxycholic acid suppresses mitochondria-dependent programmed cell death induced by sodium nitroprusside in SH-SY5Y cells. *Toxicology* 292**,** 105-112.

Dehay, B., Ramirez, A., Martinez-Vicente, M., Perier, C., Canron, M.H., Doudnikoff, E., Vital, A., Vila, M., Klein, C., Bezard, E., 2012. Loss of P-type ATPase ATP13A2/PARK9 function induces general lysosomal deficiency and leads to Parkinson disease neurodegeneration. *Proc Natl Acad Sci U S A* 109**,** 9611-9616.

Espay, A.J., Schwarzschild, M.A., Tanner, C.M., Fernandez, H.H., Simon, D.K., Leverenz, J.B., Merola, A., Chen-Plotkin, A., Brundin, P., Kauffman, M.A., Erro, R., Kieburtz, K., Woo, D., Macklin, E.A., Standaert, D.G., Lang, A.E., 2017. Biomarker-driven phenotyping in Parkinson's disease: A translational missing link in disease-modifying clinical trials. *Mov Disord* 32**,** 319-324.

Gasser, T., 2015. Usefulness of Genetic Testing in PD and PD Trials: A Balanced Review. *J Parkinsons Dis* 5**,** 209-215.

Georges, P., Boza-Moran, M.G., Gide, J., Peche, G.A., Foret, B., Bayot, A., Rustin, P., Peschanski, M., Martinat, C., Aubry, L., 2019. Induced pluripotent stem cells-derived neurons from patients with Friedreich ataxia exhibit differential sensitivity to resveratrol and nicotinamide. *Sci Rep* 9**,** 14568.

Hattingen, E., Magerkurth, J., Pilatus, U., Mozer, A., Seifried, C., Steinmetz, H., Zanella, F., Hilker, R., 2009. Phosphorus and proton magnetic resonance spectroscopy demonstrates mitochondrial dysfunction in early and advanced Parkinson's disease. *Brain* 132**,** 3285-3297.

Hockey, L.N., Kilpatrick, B.S., Eden, E.R., Lin-Moshier, Y., Brailoiu, G.C., Brailoiu, E., Futter, C.E., Schapira, A.H., Marchant, J.S., Patel, S., 2015. Dysregulation of lysosomal

morphology by pathogenic LRRK2 is corrected by TPC2 inhibition. *J Cell Sci* 128**,** 232-238.

Joyner, M.J., Paneth, N., 2019. Promises, promises, and precision medicine. *J Clin Invest* 129**,** 946-948.

Kuleshov, M.V., Jones, M.R., Rouillard, A.D., Fernandez, N.F., Duan, Q., Wang, Z., Koplev, S., Jenkins, S.L., Jagodnik, K.M., Lachmann, A., McDermott, M.G., Monteiro, C.D., Gundersen, G.W., Ma'ayan, A., 2016. Enrichr: a comprehensive gene set enrichment analysis web server 2016 update. *Nucleic Acids Res* 44**,** W90-97.

Lesage, S., Drouet, V., Majounie, E., Deramecourt, V., Jacoupy, M., Nicolas, A., Cormier-Dequaire, F., Hassoun, S.M., Pujol, C., Ciura, S., Erpapazoglou, Z., Usenko, T., Maurage, C.A., Sahbatou, M., Liebau, S., Ding, J., Bilgic, B., Emre, M., Erginel-Unaltuna, N., Guven, G., Tison, F., Tranchant, C., Vidailhet, M., Corvol, J.C., Krack, P., Leutenegger, A.L., Nalls, M.A., Hernandez, D.G., Heutink, P., Gibbs, J.R., Hardy, J., Wood, N.W., Gasser, T., Durr, A., Deleuze, J.F., Tazir, M., Destee, A., Lohmann, E., Kabashi, E., Singleton, A., Corti, O., Brice, A., French Parkinson's Disease Genetics, S., International Parkinson's Disease Genomics, C., International Parkinson's Disease Genomics Consortium, I., 2016. Loss of VPS13C Function in Autosomal-Recessive Parkinsonism Causes Mitochondrial Dysfunction and Increases PINK1/Parkin-Dependent Mitophagy. *Am J Hum Genet* 98**,** 500-513.

Li, T., Kung, H.J., Mack, P.C., Gandara, D.R., 2013. Genotyping and genomic profiling of non-small-cell lung cancer: implications for current and future therapies. *J Clin Oncol* 31**,** 1039-1049.

McNeill, A., Magalhaes, J., Shen, C., Chau, K.Y., Hughes, D., Mehta, A., Foltynie, T., Cooper, J.M., Abramov, A.Y., Gegg, M., Schapira, A.H., 2014. Ambroxol improves lysosomal

biochemistry in glucocerebrosidase mutation-linked Parkinson disease cells. *Brain* 137**,** 1481-1495.

Meyer, K., Ferraiuolo, L., Miranda, C.J., Likhite, S., McElroy, S., Renusch, S., Ditsworth, D., Lagier-Tourenne, C., Smith, R.A., Ravits, J., Burghes, A.H., Shaw, P.J., Cleveland, D.W., Kolb, S.J., Kaspar, B.K., 2014. Direct conversion of patient fibroblasts demonstrates non-cell autonomous toxicity of astrocytes to motor neurons in familial and sporadic ALS. *Proc Natl Acad Sci U S A* 111**,** 829-832.

Mortiboys, H., Aasly, J., Bandmann, O., 2013. Ursocholanic acid rescues mitochondrial function in common forms of familial Parkinson's disease. *Brain* 136**,** 3038-3050.

Mortiboys, H., Furmston, R., Bronstad, G., Aasly, J., Elliott, C., Bandmann, O., 2015. UDCA exerts beneficial effect on mitochondrial dysfunction in LRRK2(G2019S) carriers and in vivo. *Neurology* 85**,** 846-852.

Mortiboys, H., Johansen, K.K., Aasly, J.O., Bandmann, O., 2010. Mitochondrial impairment in patients with Parkinson disease with the G2019S mutation in LRRK2. *Neurology* 75**,** 2017-2020.

Mortiboys, H., Thomas, K.J., Koopman, W.J., Klaffke, S., Abou-Sleiman, P., Olpin, S., Wood, N.W., Willems, P.H., Smeitink, J.A., Cookson, M.R., Bandmann, O., 2008. Mitochondrial function and morphology are impaired in parkin-mutant fibroblasts. *Ann Neurol* 64**,** 555-565.

Papagiannakis, N., Xilouri, M., Koros, C., Stamelou, M., Antonelou, R., Maniati, M., Papadimitriou, D., Moraitou, M., Michelakakis, H., Stefanis, L., 2015. Lysosomal alterations in peripheral blood mononuclear cells of Parkinson's disease patients. *Mov Disord* 30**,** 1830-1834.

Patro, R., Duggal, G., Love, M.I., Irizarry, R.A., Kingsford, C., 2017. Salmon provides fast and bias-aware quantification of transcript expression. *Nat Methods* 14**,** 417-419.

Purcell, S., Neale, B., Todd-Brown, K., Thomas, L., Ferreira, M.A., Bender, D., Maller, J., Sklar, P., de Bakker, P.I., Daly, M.J., Sham, P.C., 2007. PLINK: a tool set for whole-genome association and population-based linkage analyses. *Am J Hum Genet* 81**,** 559-575.

Rakovic, A., Grunewald, A., Voges, L., Hofmann, S., Orolicki, S., Lohmann, K., Klein, C., 2011. PINK1-Interacting Proteins: Proteomic Analysis of Overexpressed PINK1. *Parkinsons Dis* 2011**,** 153979.

Robak, L.A., Jansen, I.E., van Rooij, J., Uitterlinden, A.G., Kraaij, R., Jankovic, J., International Parkinson's Disease Genomics, C., Heutink, P., Shulman, J.M., 2017. Excessive burden of lysosomal storage disorder gene variants in Parkinson's disease. *Brain* 140**,** 3191-3203.

Rosen, A., Zeger, S.L., 2019. Precision medicine: discovering clinically relevant and mechanistically anchored disease subgroups at scale. *J Clin Invest* 129**,** 944-945.

Schapira, A.H., Olanow, C.W., Greenamyre, J.T., Bezard, E., 2014. Slowing of neurodegeneration in Parkinson's disease and Huntington's disease: future therapeutic perspectives. *Lancet* 384**,** 545-555.

Shamir, R., Klein, C., Amar, D., Vollstedt, E.J., Bonin, M., Usenovic, M., Wong, Y.C., Maver, A., Poths, S., Safer, H., Corvol, J.C., Lesage, S., Lavi, O., Deuschl, G., Kuhlenbaeumer, G., Pawlack, H., Ulitsky, I., Kasten, M., Riess, O., Brice, A., Peterlin, B., Krainc, D., 2017. Analysis of blood-based gene expression in idiopathic Parkinson disease. *Neurology* 89**,** 1676-1683.

Smith, A.M., Depp, C., Ryan, B.J., Johnston, G.I., Alegre-Abarrategui, J., Evetts, S., Rolinski, M., Baig, F., Ruffmann, C., Simon, A.K., Hu, M.T.M., Wade-Martins, R., 2018. Mitochondrial dysfunction and increased glycolysis in prodromal and early Parkinson's blood cells. *Mov Disord* 33**,** 1580-1590.

Stelzer, G., Plaschkes, I., Oz-Levi, D., Alkelai, A., Olender, T., Zimmerman, S., Twik, M., Belinky, F., Fishilevich, S., Nudel, R., Guan-Golan, Y., Warshawsky, D., Dahary, D., Kohn, A., Mazor, Y., Kaplan, S., Iny Stein, T., Baris, H.N., Rappaport, N., Safran, M., Lancet, D., 2016. VarElect: the phenotype-based variation prioritizer of the GeneCards Suite. *BMC Genomics* 17 Suppl 2**,** 444.

Szewczyk-Krolikowski, K., Tomlinson, P., Nithi, K., Wade-Martins, R., Talbot, K., Ben-Shlomo, Y., Hu, M.T., 2014. The influence of age and gender on motor and non-motor features of early Parkinson's disease: initial findings from the Oxford Parkinson Disease Center (OPDC) discovery cohort. *Parkinsonism Relat Disord* 20**,** 99-105.

Tan, M.M.X., Malek, N., Lawton, M.A., Hubbard, L., Pittman, A.M., Joseph, T., Hehir, J., Swallow, D.M.A., Grosset, K.A., Marrinan, S.L., Bajaj, N., Barker, R.A., Burn, D.J., Bresner, C., Foltynie, T., Hardy, J., Wood, N., Ben-Shlomo, Y., Grosset, D.G., Williams, N.M., Morris, H.R., 2019. Genetic analysis of Mendelian mutations in a large UK population-based Parkinson's disease study. *Brain* 142**,** 2828-2844.

van der Brug, M.P., Singleton, A., Gasser, T., Lewis, P.A., 2015. Parkinson's disease: From human genetics to clinical trials. *Sci Transl Med* 7**,** 205ps220.

Vandoorne, T., Veys, K., Guo, W., Sicart, A., Vints, K., Swijsen, A., Moisse, M., Eelen, G., Gounko, N.V., Fumagalli, L., Fazal, R., Germeys, C., Quaegebeur, A., Fendt, S.M., Carmeliet, P., Verfaillie, C., Van Damme, P., Ghesquiere, B., De Bock, K., Van Den Bosch, L., 2019. Differentiation but not ALS mutations in FUS rewires motor neuron metabolism. *Nat Commun* 10**,** 4147.